RSC Advances

ROYAL SOCIETY OF CHEMISTRY

www.rsc.org/advances

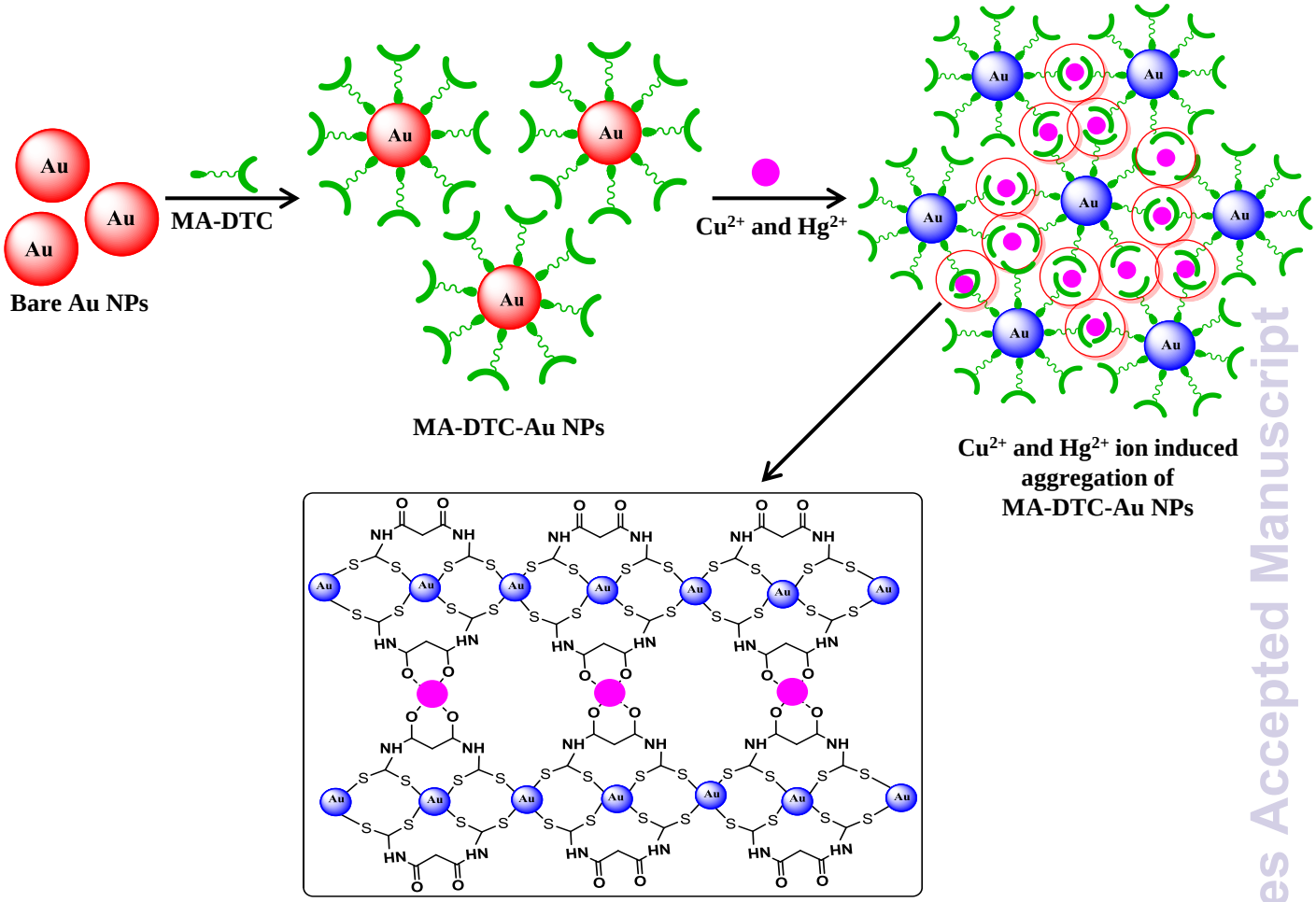

Malonamide dithiocarbamate functionalized gold nanoparticles for colorimetric sensing of Cu^{2+} and Hg^{2+} ions

Vaibhavkumar N. Mehta and Suresh Kumar Kailasa*

Department of Chemistry, S. V. National Institute of Technology, Surat-395 007, India
**Corresponding author, Phone: +91-261-2201730; Fax: +91-261-2227334*
E-mail: sureshkumarchem@gmail.com; skk@ashd.svnit.ac.in

Abstract

In this study, a colorimetric probe was developed based on the malonamide dithiocarbamate functionalized gold nanoparticles (MA-DTC-Au NPs) for simultaneous colorimetric detection of Cu^{2+} and Hg^{2+} ions. The MA-DTC-Au NPs were quickly aggregated in the presence of Cu^{2+} and Hg^{2+} ions, resulting a color change from red to blue and red-shift in their surface plasmon resonance peak (SPR) from 525 to 780 nm and to 680 nm for Cu^{2+} and Hg^{2+} ions, respectively. On the basis of this, the concentration of Cu^{2+} and Hg^{2+} ions can be visualized with the naked eyes that can be quantitatively determined by UV−visible spectroscopy. The absorption ratios A_{780nm}/A_{525nm} and A_{680nm}/A_{525nm} show linear relationships with Cu^{2+} and Hg^{2+} ions concentrations within concentration ranges from 0.01 to 5 and 0.01 to 10 μM. The detection limits are as low as 41 nM and 45 nM for Cu^{2+} and Hg^{2+} ions, respectively. The MA-DTC-Au NPs was used as a potential colorimetric prober for the rapid, selective and sensitive detection of Cu^{2+} and Hg^{2+} ions in environmental water samples (drinking, tap, canal and river water).

Keywords: MA-DTC-Au NPs, Cu^{2+} ion, Hg^{2+} ion, UV-visible spectroscopy, DLS and TEM

Introduction

Recent years, the development of selective and sensitive probe for metal ions is in great demand due to their toxicity and shown adverse effect on the human health. [1,2] Among this, mercury is one of the most ubiquitous non-biodegradable toxic element which contaminates water and soil in various compositions (inorganic salts and metal complexes).[3,4] Hg^{2+} ion can accumulate into human body *via* water or food chain due to its water solubility and passes easily through biological membranes.[5] Moreover, higher concentration of Hg^{2+} ion in body can permanently cause damage to brain, liver and the central nervous system.[6,7] On the other hand, copper is well known as the third essential transition element for the living organism which plays key role in various metabolic pathways and biological processes at certain concentrations.[8] However, excess amount of Cu^{2+} ions in human body can cause serious neurodegenerative diseases such as cirrhosis,[9] Alzheimer's disease[10] and inflammatory disorders.[11] Therefore, detection of both the metal ions is essentially required at ultra trace levels in various environmental and biological samples. In this connection, many of the sophisticated analytical techniques are readily available to quantify both the metal ions (Cu^{2+} and Hg^{2+}) in environmental samples at trace levels. Generally, these methods include atomic absorption spectroscopy (AAS),[12,13] cyclic voltammetry,[14] inductively coupled plasma mass spectrometry (ICP-MS)[15,16] and use of some organic fluorophores[17] and biomolecules.[18] Although these methods provide good sensitivity but they are expensive and often required tedious sample treatment and also limited to on-site real time *in-situ* detection of metal ions. To overcome aforesaid problem, there is a need to develop a rapid, simple and economically viable method which allows real time *in-situ* detection of both the metal ions at ultra trace levels.

The recent advancement in the field of nano-analytical science opens up new era for the development of colorimetric probes to identify different target analytes at trace levels in various environmental and biological specimens.[19] In addition, colorimetric probes based on metallic nanoparticles (Au and Ag NPs) have attracted much more attention due to their SPR changes with target analytes, which allows us to detect the analytes with naked eye and without use of costly instruments.[20-21] In this connection, Au and Ag NPs based colorimetric probe have been extensively studied to trace different target analytes due to their distinguishable physico-chemical properties and SPR.[22] The target analytes can be induced the aggregation of NPs, resulting a color change and a drastic change in their absorption spectra, which facilitates to improve the performance of UV-visible spectroscopy, just like sophisticated instruments (AAS and ICP-MS).[23] Recently, extensive efforts have been devoted for the development of organic-frame work on the surfaces of Au and Ag NPs and their uses as probes for colorimetric sensing of Cu^{2+} and Hg^{2+} ions in various environmental and biological samples. For example, Zhou *et al.* developed a colorimetric sensor for the detection of Cu^{2+} ion using 4-mercaptobenzoic acid modified Ag NPs as a probe.[24] Maity *et al.* illustrated the use of dithiocarbamate derivative of calixarene functionalized Au NPs as a colorimetric probe for the detection of Hg^{2+} ions in drinking water.[25] Tan's group described the use of mercaptopropionic acid and homocystine functionalized Au NPs in cloud point extraction for the extraction and preconcentration of Hg^{2+} ion in environmental samples and quantified by UV-visible spectroscopy.[26] Similarly, sensitive and selective colorimetric methods have been developed for the detection of Hg^{2+} ion using cyanuric acid[27]- and cysteamine[28]- capped Au NPs as probes. Most recently, thioctic acid functionalized Au NPs were used as a colorimetric sensor for the

detection of Hg^{2+} ion in lake water samples.[29] Furthermore, simple colorimetric method is developed to detect Cu^{2+} ions using unmodified Au NPs as a probe *via* copper(I)-catalyzed click chemistry.[30] Moreover, our group also described the uses of dopamine dithiocarbamate[31] and dithiocarbamate-modified 4′-aminobenzo-18-crown-6[32] capped Au NPs as probes for colorimetric detection of Cu^{2+} ion and Pb^{2+} ion in environmental samples. Generally, heavy metal ions (Cu^{2+}, Hg^{2+}, Pb^{2+} and Cd^{2+} etc.) usually coexist in nature and widely distributed at trace levels in ambient air, water, soil, food, and biological systems. Simultaneous detection of multiple metal ions at trace levels in various environmental and biological samples using single probe is in great demand. Since, discriminative detection of single metal ion over other similar metal ions is still challenging, since heavy metal ions show similar coordination ability with the chelating agents. Therefore, it is of continuing interest to develop novel probe for discriminative detection of single metal ions over other metal ions with reduced sample preparations.

Up to date, very limited reports are available in terms of simultaneous detection of metal ions using the single probe based on the Au and Ag NPs. In this connection, Li *et al.* developed a simple and selective method for ultra sensitive detection of Cu^{2+} and Hg^{2+} ions based on surface-enhanced raman scattering using cysteine-functionalized Ag NPs.[33] Alizadeh *et al.* developed a colorimetric probe for the detection of Cu^{2+} and Ag^{+} ions using pyridines-functionalized Au NPs as a probe.[34] Dou's group synthesized homocysteine-functionalized Ag NPs for colorimetric sensing of Cu^{2+} ion and Lidocaine hydrochloride in water and biological samples.[35] Furthermore, Liu *et al.* illustrated the use of Ag NPs as a selective and sensitive fluorescent probe for the detection of Cu^{2+} and Hg^{2+} ions in mineral water samples.[36] Ye's group described the use of peptide (CALNNDHHHHHH)

functionalized Au NPs for parallel colorimetric detection of Cd^{2+}, Ni^{2+} and Co^{2+} ions in river water samples.[37] Jiang *et al.* demonstrated the use of protein functionalized Au NPs as a probe for simultaneous colorimetric detection of Hg^{2+}, Pb^{2+} and Cu^{2+} ions in water samples.[38] Moreover, Annadhasan *et al.* developed green synthetic approaches for preparation of Au and Ag NPs and used as probes for simultaneous detection of Hg^{2+}, Pb^{2+} and Mn^{2+} ions in water samples.[39] Recently, Anthony's group synthesized Ag NPs from plant extracts (neem leaf, mango leaf, green tea and pepper seed) and used as a probe for colorimetric detection of multiple metal ions (Hg^{2+}, Zn^{2+}, Pb^{2+}) over a wide pH range.[40] The same group describes the use of *N*-(2-hydroxybenzyl)-valine and *N*-(2-hydroxybenzyl)-isoleucine functionalized Ag NPs as a colorimetric probe for simultaneous detection of Cd^{2+}, Hg^{2+} and Pb^{2+} ions in aqueous solution at ppm level.[41] These reports demonstrated that the potentiality of Au and Ag NPs as colorimetric probes to detect metal ions in various environmental and biological samples. Inspired by these works, we decided to functionalize Au NPs with malonamide dithiocarbamate that can act as a distinct probe for simultaneous colorimetric detection of metal ions.

In this study, we developed a rapid, simple, sensitive and selective method for dual colorimetric detection of Cu^{2+} and Hg^{2+} ions using MA-DTC-Au NPs as a probe. The MA-DTC-Au NPs were quickly aggregated in the presence of Cu^{2+} and Hg^{2+} ions, resulting a color change from red to blue. This aggregation is attributed to the complex formation of both metal ions with carbonyl group of MA-DTC-Au NPs (Scheme 1).

Experimental

Chemicals and materials

Hydrogen tetrachloroaurate hydrate ($HAuCl_4 \cdot xH_2O$), tris(hydroxymethyl) aminomethane (Tris), metal salts ($Zn(NO_3)_2 \cdot 6H_2O$, $Mn(NO_3)_2 \cdot 4H_2O$, $Co(NO_3)_2 \cdot 6H_2O$, $Pb(NO_3)_2$, $Cd(NO_3)_2 \cdot 4H_2O$, $Cu(NO_3)_2 \cdot 3H_2O$, $Hg(NO_3)_2 \cdot H_2O$, $FeCl_2 \cdot 4H_2O$, $Mg(NO_3)_2 \cdot 6H_2O$, $NiSO_4 \cdot 6H_2O$, $FeCl_3 \cdot 6H_2O$, $Cr(NO_3)_2.6H_2O$, $CaCl_2 \cdot 2H_2O$, $AlCl_3$) were purchased from Sigma-Aldrich, USA. Carbon disulfide, acetic acid, methanol, ethylenediaminetetraacetic acid (EDTA) and hydrochloric acid were purchased from Merck Ltd., India. Trisodium citrate dehydrate and potassium thiocyanate (SCN^-) were obtained from SD Fine Chemicals Ltd., India. Malonic acid was purchased from Loba Chemie Pvt. Ltd., India. All chemicals were of analytical grade and used without further purification. All the samples were prepared by using Milli-Q-purified water.

Synthesis of MA-DTC-Au NPs

The Au NPs were prepared by citrate reduction of $HAuCl_4$.[42] Briefly, 100 mL aqueous solution of 1 mM $HAuCl_4$ was brought to a refluxed condition with stirring in a round bottom flask. Then, 38.8 mM of trisodium citrate (10 mL) was added rapidly to the above solution. The solution was refluxed for another 15 min with continuous stirring. The color of the solution was turned into wine red from the pale yellow which confirms the formation of Au NPs with the average diameter of 10 nm. Malonamide dithiocarbamate (MA-DTC) was synthesized by reacting the equimolar mixture of malonamide (0.01 M) and CS_2 (0.01 M) in methanolic KOH at 40 ^oC for 30 minutes. The resulting product was filtered and recrystallized from ethanol and then acidified with dilute AcOH. To functionalize Au NPs with MA-DTC, 300 µL of MA-DTC was added into 20 mL of Au NPs and then stirred for 2 h to make sure the MA-DTC molecular assembly on the surface of Au NPs. Supporting Information of

Figure S1 shows the schematic illustration for the synthesis of MA-DTC and functionalization of Au NPs with MA-DTC.

Colorimetric detection of Cu^{2+} and Hg^{2+} ions

For the colorimetric detection of Cu^{2+} and Hg^{2+} ions, 100 µL of Tris-HCl buffer solution (pH 8) was mixed with 800 µL of MA-DTC-Au NPs into 4 mL sample vials and then 100 µL of different concentrations of both metal ions (Cu^{2+} and Hg^{2+} ions) were added. The mixture was vortexed for 30 s and the color changes were observed from red to blue with naked eye. UV-visible absorption spectra of the above solutions were measured by using a Maya Pro 2000 spectrophotometer.

Determination of Cu^{2+} and Hg^{2+} ions in environmental water samples

To confirm the practical applicability of MA-DTC-Au NPs as colorimetric probe for Cu^{2+} and Hg^{2+} ions, environmental samples (drinking, tap, canal and river water) from different sources were collected. i.e., drinking and tap water (Research laboratory, SVNIT, Surat), canal water (Agriculture canal, Surat, India) and river water (Tapi river, Surat, India). The collected samples were spiked with the different concentration of Cu^{2+} and Hg^{2+} ions (0.5, 5 and 50 µM) after filtered through 0.45 µm membrane and then analyzed by aforesaid procedure.

Instrumentation

UV-visible spectra were measured with Maya Pro 2000 spectrophotometer (Ocean Optics, USA) at room temperature. Fourier transform infrared (FT-IR) spectra were recorded on a Perkin Elmer (FT-IR spectrum BX, Germany). ^1H NMR spectra were recorded on a Varian 400 MH_Z instrument (USA). TEM samples were prepared

by dropping 10-15 μL NPs colloidal solution onto a copper grid (3 mm, 200 mesh) coated with carbon film, allowed it to dried up and analyzed with Tecnai 20 (Philips, Holland) transmission electron microscope at an acceleration voltage of 100 kV. DLS measurements were performed by using Zetasizer Nano ZS90 (Malvern, UK).

Results and discussion

Characterization of MA-DTC-Au NPs

The MA-DTC-Au NPs were characterized by the various spectroscopic (UV-visible, FT-IR, ^{1}H NMR) techniques. DLS and TEM analysis were carried out to investigate the size and morphology of MA-DTC-Au NPs. Figure 1 shows the UV-visible spectra of bare Au NPs before and after functionalization with MA-DTC. The bare Au NPs shows the characteristic SPR peak centered at 520 nm. After functionalization with MA-DTC, the SPR peak intensity was slightly red shifted to 525 nm which confirms the successful attachment of MA-DTC ligand on the surfaces of Au NPs *via* S-Au 'zero length' covalent bond.[43] The color of MA-DTC-Au NPs is remained ruby red as bare Au NPs, indicating that MA-DTC-Au NPs are still in dispersion state. Supporting Information of Figure S2 shows the FT-IR spectra of pure malonamide, MA-DTC and MA-DTC-Au NPs, respectively. FT-IR spectrum of pure malonamide shows the characteristic bands at 3317 and 3163 cm^{-1} due to the N–H asymmetric and symmetric stretching modes of $–NH_2$ group, respectively. The peak at 2796 cm^{-1} was attributed to the –C-H starching of methylene group. The strongest absorption peak of C=N stretching mode was observed at 1404 cm^{-1}. The C=O stretching was observed at 1670 cm^{-1}. As shown in Supporting Information of Figure S2b, MA-DTC exhibit new peaks at 1063, 1257 and 2823 cm^{-1}, which corresponded to -C-S, –CS-NH- and -S-H groups stretching and bending vibrations, respectively.

Importantly, two bands of $–NH_2$ groupat 3317 and 3163 cm^{-1} are observed at 3387 cm^{-1}, which indicates that $–NH_2$ group is in the formation of MA-DTC. Moreover, -SH group stretching and bending vibrations at 2823 cm^{-1} were disappeared in FT-IR spectrum of MA-DTC-Au NPs, confirming that the successful attachment of MA-DTC onto the surfaces of Au NPs surface.

Supporting Information of Figure S3 shows the ^1H NMR spectra of pure malonamide, MA-DTC and MA-DTC-Au NPs. The peaks at 7.4 and 2.9 δ ppm correspond to the protons of $–NH_2$ and methylene groups in malonamide, respectively. No enol form has been observed in DMSO solution in ^1H NMR spectrum of malonamide.[44] The appearance of a new peak at 2.9 δ ppm confirms the proton peak of–SH group of MA-DTC (Supporting Information of Figure S3b). The peak at 3.4 δ ppm was assigned to methylene group. Furthermore, the proton peaks at 7.5 and 6.9 δ ppm correspond to the protons of amino group in MA-DTC (Supporting Information of Figure S3b). As shown in Supporting Information of Figure S3c, ^1H NMR spectrum of MA-DTC-Au NPs did not exhibit any proton peaks, which represents the up-field chemical shift of all the protons in MA-DTC-Au NPs.

DLS was carried out to confirm the dispensability and hydrodynamic diameter of bare Au NPs and MA-DTC-Au NPs. Figure 2a shows the DLS of bare Au NPs which indicate that before surface modification, the bare Au NPs had an average hydrodynamic diameter of ~5 nm. However, the average hydrodynamic diameter is increased to ~25 nm, which is due to MA-DTC molecular assembly on the surface of Au NPs (Figure 2b). As shown in Figure 3a, TEM image of MA-DTC-Au NPs revealed that the functionalized Au NPs were uniform, spherical in shape and well separated from each other with an average size of ~20 nm, which is well agreed with DLS data.

MA-DTC-Au NPs as a probe for colorimetric sensing of Cu^{2+} and Hg^{2+} ions

To investigate the selectivity of MA-DTC-Au NPs towards different metal ions, 100 µL of different metal ions (Cd^{2+}, Co^{2+}, Cr^{3+}, Cu^{2+}, Fe^{2+}, Fe^{3+}, Hg^{2+}, Mn^{2+}, Mg^{2+}, Na^{+}, Ni^{2+}, Pb^{2+}, Zn^{2+}, Al^{3+}, 100 µM) were added individually into the 800 µL of MA-DTC-Au NPs at Tris-HCl buffer pH 8.0 and their UV-visible absorption spectra were recorded. Figure 4a shows the UV-visible spectra of MA-DTC-Au NPs in presence of different metal ions. It can be observed that only Cu^{2+} and Hg^{2+} ions resulted in a substantial change in their SPR peak from 525 to 780 and to 680 nm for Cu^{2+} and Hg^{2+} ions, respectively. The shift in their SPR peak could be observed by naked eye as a color change from red to blue which confirms the aggregation of MA-DTC-Au NPs in presence of Cu^{2+} and Hg^{2+} ions (Figure 4b). The other metal ions did not influence the UV-visible spectra and color change of MA-DTC-Au NPs, indicating that only Cu^{2+} and Hg^{2+} ions are induced MA-DTC-Au NPs aggregations. Supporting Information of Figure S4 represents the sensing response of MA-DTC-Au NPs towards different metal ions expressed in terms of absorption ratios A_{780nm}/A_{525nm} and A_{680nm}/A_{525nm} for Cu^{2+} and Hg^{2+} ions, respectively.

Sensing mechanism

As shown in Supporting Information of Figure S1, malonamide contains amino ($-NH_2$) and carbonyl (-C=O) groups. Generally, malonamide acts as a bidentate ligand and its carbonyl groups can provide sites for metal complexes, since $-NH_2$ group is already involved in the MA-DTC formation. At pH 8.0, these negatively charged carbonyl groups can effectively act as sites for coordination covalent bonds with metal ions.[45] As a result,the positively charged metal ions stabilize the negative

charge on the carbonyl oxygen atoms and form coordinate covalent bonds with Cu^{2+} and Hg^{2+} ions at pH 8.0, resulting a higher degree of MA-DTC-Au NPs aggregations. The another possible mechanism is also attributed for Hg^{2+} ion-induced MA-DTC Au NPs aggregation. Since, MA-DTC molecule can easily displace from the surfaces of Au NPs due to complex formation between MA-DTC and Hg^{2+} ions, promoting Au NPs to assemble into arrays through the bare surfaces by dipole–dipole interaction.[25,46] Hg^{2+} ions shows high affinity towards –SH group over the Au NPs surface due to its lower solubility product constant (K_{sp}) of Hg-S (4.0×10^{-53}) as compare to other metal ions-sulfur complex.[29,47] To support this mechanism, complexation behavior of MA-DTC with Cu^{2+} and Hg^{2+} ions were also investigated. Supporting Information of Figure S5 shows the UV-visible spectra of pure malonamide, MA-DTC, MA-DTC-Cu^{2+} complex and MA-DTC-Hg^{2+} complex. The new absorbance peak was observed around 300 nm in case of MA-DTC which is due to formation of dithiocarbamate groups at the end of primary amines of malonamide molecule. After addition of Hg^{2+} into 1 mM of MA-DTC solution, the peak of dithiocarbamate group is suddenly decreased due to the formation of Hg-S complex whereas no noticeable change is observed after addition of Cu^{2+} ions into 1 mM of MA-DTC solution. To confirm the role of MA-DTC on the surface of Au NPs, comparison study was carried out by functionalizing Au NPs with malonic acid containing similar 1,3 carbonyl group as malonamide. Supporting Information of Figure S6a shows the UV-visible absorption spectra of Au NPs functionalized with different concentrations of malonic acid ranging from 1.0 to 50 mM. These results suggested that higher concentration of malonic acid (45 mM) is required to functionalize Au NPs as compare to MA-DTC (1.0 mM). This may be attributed to the presence of electron rich hydroxyl group in malonic acid which further facilitate

the reduction of Au NPs while thiol group of MA-DTC can easily attached on the surface of Au NPs *via* zero-length covalent Au-S bond. Supporting Information of Figure 6b and c shows the UV-visible spectra of malonic acid functionalized Au NPs in presence of 100 µM Cu^{2+} and Hg^{2+} ions, respectively. It is clearly observed that 100 µM of Cu^{2+} ion induced the aggregation of malonic acid capped Au NPs with 50 mM malonic acid due to complex formation between Cu^{2+} ion and two negatively charged carbonyl groups. Moreover, Hg^{2+} ions moderately induced the aggregation of malonic acid capped Au NPs even at 50 mM concentration of malonic acid due to unavailability of -SH groups to form Hg-S complex, indicating that MA-DTC molecules on Au NPs surfaces play key role to make coordinate covalent bonds with Hg^{2+}, which yields the aggregation of MA-DTC Au NPs. To confirms this, we studied the DLS and TEM of MA-DTC-Au NPs in presence of Cu^{2+} and Hg^{2+} ions. Figure 2c and d shows the DLS of MA-DTC-Au NPs in the presence of Cu^{2+} and Hg^{2+} ions (100 µM) at pH 8.0. The average hydrodynamic diameter MA-DTC-Au NPs was increased from ~ 25 to ~ 240 nm and to ~220 nm by the addition of Cu^{2+} and Hg^{2+} ions, which confirms that both metal ions are induced the aggregation of MA-DTC Au NPs. Figure 3b and c shows the TEM images of MA-DTC-Au NPs after addition of 100 µM Cu^{2+} and Hg^{2+} ions. These results clearly revealed that Cu^{2+} and Hg^{2+} ions-induced the aggregation of MA-DTC-Au NPs due to the formation of complexes with MA-DTC Au NPs.

Effect of pH

To find the suitable pH range for the colorimetric detection of Cu^{2+} and Hg^{2+} ions, 100 µL of tris-HCl buffer with different pH range (2.0-12) was added into MA-DTC-Au NPs. Supporting Information of Figure S7 shows the absorption ratio

(A_{680nm}/A_{525nm}) of MA-DTC-Au NPs in the pH range of 2.0-12. It can be observed that intra molecular hydrogen bonding was formed between malonamide molecules *via* carbonyl groups below pH 7.0 which causes the partial aggregation of MA-DTC-Au NPs without addition of analyte.[29] Furthermore, the dithiocarbamate anions get protonated due to the breaking of Au-S bond in acidic pH range (pH <4.0), leads to the aggregation of MA-DTC-Au NPs.[25] The absorption ratios were constant in the pH range 8.0–12, which indicated the stability of MA-DTC-Au NPs. The effect of pH on Cu^{2+} and Hg^{2+} ions induced aggregation of MA-DTC-Au NPs is also shown in Supporting Information of Figure S7. The absorption ratios (A_{780nm}/A_{525nm} and A_{680nm}/A_{525nm}) were higher at pH 8.0 for Cu^{2+} and Hg^{2+} ions, which indicates that both metal ions showed high affinity to make complex with MA-DTC-Au NPs at this pH. At pH > 9.0, Cu^{2+} and Hg^{2+} ions did not induce the aggregation of MA-DTC-Au NPs due to formation of metal hydroxide. Therefore, pH 8.0 was selected as optimal pH for colorimetric sensing of Cu^{2+} and Hg^{2+} ions using MA-DTC-Au NPs as a probe.

Analytical evaluation of MA-DTC-Au NPs as colorimetric probe for Cu^{2+} and Hg^{2+} ions

To evaluate the potentiality of MA-DTC-Au NPs as a colorimetric probe for Cu^{2+} and Hg^{2+} ions, UV-visible spectra of MA-DTC-Au NPs were measured in presence of different concentration of Cu^{2+} and Hg^{2+} ions separately under optimized condition. As shown in Figure 5b and 6b, the color of the solutions were changed gradually from red to purple and finally blue upon increasing concentration of Cu^{2+} and Hg^{2+} ions from 0.01 to 100 μM, which can be observed by the naked eye. Furthermore, the SPR peak (at 525 nm) of MA-DTC-Au NPs was gradually decreased and new peaks at 780 and 680 nm were gradually increased for Cu^{2+} and Hg^{2+} ions

with increasing concentration of both ions from 0.01 to 100 μM (Figure 5a and 6a). These results suggest that the higher concentration of Cu^{2+} and Hg^{2+} ions can be induced a higher degree of aggregation of MA-DTC-Au NPs. Furthermore, calibration graphs were constructed using intensities of absorption ratios at A_{780nm}/A_{525nm} and A_{680nm}/A_{525nm} and the logarithm concentrations in the range of 0.01 to 5 μM and 0.01 to 10 μM for Cu^{2+} and Hg^{2+} ions, respectively (Supporting Information of Figure S8). The linear relationship was obtained with the equations y = 1.4885+0.1447 log $C[Cu^{2+}]$ and y = 1.1763+0.1332 log $C[Hg^{2+}]$ with the correlation coefficient value (R^2) of 0.9973, 0.9970 for Cu^{2+} and Hg^{2+} ions, respectively. The limit of detection (LOD) was calculated using the formula, LOD = 3 × sb/S (in which, sb = standard deviation of blank signal (n=3) and S = slope of the concentration peak intensity of calibration curve). The limit of detection was found to be 41 and 45 nM for Cu^{2+} and Hg^{2+} ions, respectively. It was observed that the obtained LOD is is somewhat similar to other reported methods for colorimetric detection of Cu^{2+} and Hg^{2+} ions by using functionalized Au and Ag NPs.[29,39,48,50-51] Table 1 shows the comparison of present method with the other reported NPs assisted UV-Visible,[24,25,27-30,37-39] cloud point extraction,[26] surface enhanced raman scattering,[33] plasmon resonance scattering[35] and fluorescence[36] methods for the detection of Cu^{2+} and Hg^{2+} ions. It was observed that the LOD of the present method is not comparable with the LOD value of NPs assisted surface enhanced raman scattering, plasmon resonance scattering and fluorescence methods due to their high sensitivity than the NPs assisted UV-visible methods.

Interference study

The interference study was carried out to investigate the influence of other metal ions on Cu^{2+} and Hg^{2+} ions binding to MA-DTC-Au NPs. Different metal ions

(Cd^{2+}, Co^{2+}, Cr^{3+}, Fe^{2+}, Fe^{3+}, Mn^{2+}, Mg^{2+}, Na^{+}, Ni^{2+}, Pb^{2+}, Zn^{2+} and Al^{3+}) were added in to MA-DTC-Au NPs at 100 μM in the presence of Cu^{2+} and Hg^{2+} ions at the concentration of 50 μM. As shown in Supporting Information of Figure S9, the change in SPR peak was only observed after addition of Cu^{2+} and Hg^{2+} ions individually in the MA-DTC-Au NPs contains the mixture of different metal ions. This indicates that other metal ions did not interfere with MA-DTC Au NPs, indicating that this probe can be use for simultaneous detection of Cu^{2+} and Hg^{2+} ions in environmental samples.

Co-existence study for Cu^{2+} and Hg^{2+} ions in presence of masking agents

The results revealed that MA-DTC-Au NPs were successfully utilized for the simultaneous detection of Cu^{2+} and Hg^{2+} ions. However, metal ions (Cu^{2+} and Hg^{2+}) are usually coexisting in various environmental and biological samples. Therefore, masking agents were used in order to achieve the selective simultaneous detection of each metal ion in presence of another metal ion. EDTA was used as masking agent for the Cu^{2+} ions to minimize the interference of the Cu^{2+} ions as it forms the stable complex with the EDTA.[49] As shown in Figure 7a, absorption ratio (A_{780nm}/A_{525nm}) of MA-DTC-Au NPs in presence of Hg^{2+} (100 μM) is almost same as that of only Hg^{2+} after addition of 100 μM of EDTA, whereas Cu^{2+} did not induce the aggregation of MA-DTC-Au NPs in presence of EDTA. Furthermore, SCN^{-} is used as masking agent for Hg^{2+} ion, since it has greater stability constant with Hg^{2+} ions and showed poor coordination ability with Cu^{2+} ion.[33] Figure 7b shows the Cu^{2+} ion successfully induces the aggregation of MA-DTC-Au NPs even in the presence of Hg^{2+} ion by using SCN^{-} as a masking agent.

The applicability of MA-DTC-Au NPs was also evaluated by addition of both the analytes at different concentration ratios (0:100 μM for Hg^{2+}:Cu^{2+} and 100:0 μM

for Hg^{2+}:Cu^{2+}) at the interval of 5 μM concentrations. As shown in Figure 7c, the SPR peak of MA-DTC-Au NPs was red shifted towards 780 nm from 680 nm with the solely addition of different concentrations of Cu^{2+} ions ranging from 0 to 100 μM in the Hg^{2+} ions different concentrations. The results revealed that Cu^{2+} ion induces higher degree of aggregation of MA-DTC-Au NPs as compare to Hg^{2+} ions because Cu^{2+} ions forms more stable complex with carbonyl groups of MA-DTC-Au NPs. These results revealed that MA-DTC Au NPs can be used as a probe for discriminative detection of Hg^{2+} over Cu^{2+} and of Cu^{2+} over Hg^{2+} using EDTA and SCN-as masking agents.

Application of MA-DTC-Au NPs as colorimetric probe in water samples

To evaluate the practical applicability of MA-DTC-Au NPs as colorimetric probe, different concentrations of Cu^{2+} and Hg^{2+} ions (0.5, 5 and 50 μM) were spiked with the water samples (drinking, tap, canal and river water) and then analyzed by aforementioned procedure. Results from the determination of both ions from various water samples are shown in Table 2 (n=3 for each concentration). These results revealed that the present method shows good recoveries in the range of 97.61% - 99.40% and 96.43% - 99.79%, with the % RSD values 1.01% - 2.70% and 1.04% - 2.72% for Cu^{2+} and Hg^{2+} ions in drinking, tap, canal and river water samples. Therefore, the present method could be used for discriminative detection of Cu^{2+} over Hg^{2+}/other metal ions and Hg^{2+} over Cu^{2+}/other metal ions in environmental samples with good accuracy and precision.

Conclusions

In summary, a colorimetric probe for simultaneous detection of Cu^{2+} and Hg^{2+} ions using MA-DTC-Au NPs was proposed. MA-DTC-Au NPs were quickly aggregated in the presence of Cu^{2+} and Hg^{2+} ions, resulting in a color change from red to blue. Quantification of Cu^{2+} and Hg^{2+} ions could be monitored by the colorimetric response of MA-DTC-Au NPs that can be observed by naked eye. The absorption ratios A_{780nm}/A_{525nm} and A_{680nm}/A_{525nm} were linear with the concentration of Cu^{2+} and Hg^{2+} ions in the range of 0.01 to 5 and 0.01 to 10 μM, respectively. Therefore, MA-DTC-Au NPs can be used as a potential colorimetric probe for the rapid, selective and sensitive detection of Cu^{2+} and Hg^{2+} ions in environmental samples.

Acknowledgement

We gratefully acknowledge the Director, SVNIT for providing all the facilities to carry out this work. We also thank Department of Science and Technology, India for providing UV-visible spectrophotometer under Fast-track Young Scientist Program (SR/FT/CS-54/2010). We thank Prof. Z.V.P. Murthy and Mr. Chetan Patel, Chemical Engineering Department, SVNIT, Surat, India for providing DLS measurements.

References

1. D. W. Domaille, E. L. Que and C. J. Chang, *Nat. Chem. Biol.*, 2008, **4**, 168.
2. P. G. Georgopoulos, A. Roy, M. J. Yonone-Lioy, R. E. Opiekun and P. J. Lioy, *J. Toxicol. Env. Heal. B*, 2001, **4**, 341.
3. A. H. Stern, *Environ. Res.*, 2005, **98**, 133.
4. P. B. Tchounwou, W. K. Ayensu, N. Ninashvili and D. Sutton, *Environ. Toxicol.,* 2003, **18**, 149.

5. Y. Fan, Y. F. Long and Y. F. Li, *Anal. Chim. Acta*, 2009, **653**, 207.
6. S. Yoon, A. E. Albers, A. P. Wong and C. J. Chang, *J. Am. Chem. Soc.,* 2005, **127**, 16030.
7. E. M. Nolan and S. J. Lippard, *Chem. Rev.,* 2008, **108**, 3443.
8. S. P. Wu, R. Y. Huang and K. J. Du, *Dalton Trans.,* 2009, **24**, 4735.
9. B. P. Zietz, H. H. Dieter, M. Lakomek, H. Schneider, B. Keßler- Gaedtke and H. Dunkelberg, *Sci. Total Environ.*, 2003, **302**, 127.
10. K. J. Barnham, C. L. Masters, A. I. Bush, *Nat. Rev. Drug Discov*., 2004, **3**, 205.
11. A. E. Fisher and D. P. Naughton, *Curr. Drug Delivery,* 2005, **2**,261.
12. R. A. Bartsch, E. Chapoteau, B. P. Czech, J. Krzykawski, A. Kamar and T. W. Robison, *J. Org. Chem.,* 1994, **59**, 616.
13. M. Chan and S. Huang, *Talanta,* 2000, **51**, 373.
14. M. A. Nolan and S. P. Kounaves, *Anal. Chem*., 1999, **71**, 3567.
15. W. Yang, D. Jaramillo, J. J. Gooding, D. B. Hibbert, R. Zhang, G. D. Willett and K. J. Fisher, *Chem. Commun*., 2001, **37**, 1982.
16. N. Burford, M. D. Eelman, D. E. Mahony and M. Morash, *Chem. Commun.*, 2003, **39**, 146.
17. X. Guo, X. Qian and L. Jia, *J. Am. Chem. Soc.*, 2004, **126**, 2272.
18. S.V. Wegner, A. Okesli, P. Chen and C. He, *J. Am. Chem. Soc.,* 2007, **129**, 3474.
19. H. N. Kim, W. X. Ren, J. S. Kim and J. Yoon, *Chem. Soc. Rev.*, 2012, **41**, 3210.
20. T. T. Lou, Z. P. Chen, Y.Q. Wang, and L.n Chen, *ACS Appl. Mater Interfaces*, 2011, **3**, 1568.
21. J. S. Lee, P. A. Ulmann, M. S. Han and C. A. Mirkin, *Nano Lett.*, 2008, **8**, 529.
22. R. Jin and G. Wu, Z. Li, J. *Am. Chem. Soc*., 2003, **125**, 1643.

23. U. Kreibig, M. Vollmer and J. P. Toennies, Optical Properties of Metal Clusters, Springer-Verlag, Berlin, 1995.

24. Y. Zhou, H. Zhao, Y. He, N. Ding and Q. Cao, *Colloid and Surface A*, 2011, **391**, 179.

25. D. Maity, A. Kumar, R. Gunupuru and P. Paul, *Colloids Surf., A*, 2014, **455**, 122.

26. Z. Tan, J. Liu, R. Liu, Y. Yin and G. Jiang, *Chem. Commun.*, 2009, **45**, 7030.

27. Z. Liu, J. Hua, S. Tong, Q. Cao and H. Yuan, *Spectrochim. Acta, Part A*, 2012, **97**, 737.

28. Y. Ma, L. Jiang, Y. Mei, R. Song, D. Tian and H. Huang, *Analyst*, 2013, **138**, 5338.

29. D. Su, X. Yang, Q. Xia, F. Chai, C. Wang and F. Qu, *RSC Adv*., 2013, **3**, 24618.

30. Q. Shen, W. Li, S. Tang, Y. Hu, Z. Nie, Y. Huang and S. Yao, *Biosens. Bioelectron.*, 2013, **41**, 663.

31. V. N. Mehta, M. A. Kumar and S. K. Kailasa, *Ind. Eng. Chem. Res.*, 2013, **52**, 4414.

32. V. N. Mehta, J. N. Solanki and S. K. Kailasa, *Microchim. Acta*, 2014, **181**, 1905.

33. F. Li, J. Wang, Y. Lai, C. Wu, S. Sun, Y. He and H. Ma, *Biosens. Bioelectron.*, 2013, **39**, 82.

34. A. Alizadeh, M. M. Khodaei, Z. Hamidi and M. Shamsuddin, *Sens. Actuators, B*, 2014, **190**, 782.

35. Y. Dou, X. Yang, Z. Liu and S. Zhu, *Colloid and Surface A*, 2013, **423**, 20.

36. J. Liu, X. Ren, X. Meng, Z. Fang and F. Tang, *Nanoscale*, 2013, **5**, 10022.

37. M. Zhang, Y. Q. Liu and B. C. Ye, *Analyst*, 2012, **137**, 601.

38. Y. Guo, Z. Wang, W. Qu, H. Shao and X. Jiang, *Biosens. Bioelectron.*, 2011, **26**, 4064.

39. M. Annadhasan, T. Muthukumarasamyvel, V. R. Sankar Babu and N. Rajendiran, *ACS Sustainable Chem. Eng.*, 2014, **2**, 887.

40. D. Karthiga and S. P. Anthony, *RSC Adv.*, 2013, **3**, 16765.

41. V. Vinod Kumar and S. P. Anthony, *Sens. Actuators, B*, 2014, **191**, 31.

42. P. C. Lee and D. Meisel, *J. Phys. Chem.,* 1982, **86**, 3391.

43. S. Y. Lin, Y. T. Tsai, C. C. Chen, C. M. Lin and C. H. Chen, *J. Phys. Chem. B*, 2004, **108**, 2134.

44. M. M. Schiavoni, H. G. Mack, S. E. Ulic and C. O. D. Ve´dova, *Spectrochim. Acta, Part A*, 2000, **56**, 1533.

45. S. D. Beukeleer, H. O. Desseyn, S. P. Perlepes and E. M. Zoupa, *Transition Met. Chem.*, 1994, **19**, 468.

46. D. Liu, W. Qu, W. Chen, W. Zhang, Z. Wang and X. Jiang, *Anal. Chem.*, 2010, **82**, 9606.

47. J. A. Dean and N. A. Lange, *Handbook of chemistry*, McGraw-Hill, 1999.

48. G. Sener, Lokman Uzun and Adil Denizli, *Anal. Chem.*, 2014, **86**, 514.

49. C. C. Huang, Y. L. Hung, T. M. Hsiung, Y. Y. Chen, Y. F. Huang, *J. Phys. Chem. C*, 2010, **114**, 16329.

50. M. Zhang, H. N. Le, X. Q. Jiang, S. M. Guo, H. J. Yu and B. C. Ye, *Talanta*, 2013, **117**, 399.

51. L. J. Miao, J. W. Xin, Z. Y. Shen, Y. J. Zhang, H. Y. Wang and A. G. Wu, *Sens. Actuators, B*, 2013, **176**, 906.

Figure captions

Scheme 1. Schematic representation of Cu^{2+} and Hg^{2+} ions-induced MA-DTC-Au NPs aggregation.

Figure 1. UV-visible spectra of bare Au NPs and MA-DTC-Au NPs. Inset picture shows bare Au NPs and MA-DTC-Au NPs.

Figure 2. DLS of (a) bare Au NPs (b) MA-DTC-Au NPs and aggregation of MA-DTC-Au NPs induced by the addition of 100 μM (c) Cu^{2+} and (d) Hg^{2+} ions.

Figure 3. TEM images of (a) MA-DTC-Au NPs and aggregation of MA-DTC-Au NPs induced by the addition of 100 μM (c) Cu^{2+} and (d) Hg^{2+} ions.

Figure 4. UV-visible absorption spectra of MA-DTC-Au NPs upon the addition of different metal ions (Al^{3+}, Ca^{2+}, Cd^{2+}, Co^{2+}, Fe^{2+}, Fe^{3+}, Mg^{2+}, Mn^{2+}, Ni^{2+}, Pb^{2+}, Zn^{2+}, Cu^{2+} and Hg^{2+}). (b) Photographic images of MA-DTC-Au NPs in the presence of various metal ions.

Figure 5. (a) UV-visible absorption spectra of MA-DTC-Au NPs with different concentrations of Cu^{2+} in the range of 0.01 to 100 μM (b) visual color change of MA-DTC-Au NPs with the addition of different concentrations of Cu^{2+} ranging from 0.01 to 100 μM.

Figure 6. (a) UV-visible absorption spectra of MA-DTC-Au NPs with different concentrations of Hg^{2+} in the range of 0.01 to 100 μM (b) visual color change of MA-DTC-Au NPs with the addition of different concentrations of Hg^{2+} ranging from 0.01 to 100 μM.

Figure 7. (a) UV-visible absorption ratio ($A_{780\ nm}/A_{525\ nm}$) of MA-DTC-Au NPs after addition of 100 μM Cu^{2+} and Hg^{2+} ions without EDTA (black bar) and with EDTA (blue bar), (b) UV-visible absorption ratio ($A_{680\ nm}/A_{525\ nm}$) of MA-DTC-Au NPs after addition of 100 μM Cu^{2+} and Hg^{2+} ions without SCN^- (black bar) and with SCN^- (red bar) and (c) UV-visible absorption spectra of MA-DTC-Au NPs in presence of mixture Cu^{2+} and Hg^{2+} ions in different concentrations (0:100 mM Cu^{2+}: Hg^{2+} to 100:0 mM Cu^{2+}: Hg^{2+}) with 5 mM concentration intervals.

Table 1. Comparison of MA-DTC-Au NPs as colorimetric probe for the detection of Cu^{2+} and Hg^{2+} with the other NPs-based reported methods.

NPs	Capping agent	Size (nm)	Analytes	LOD (M)	Detection method	Reference
Ag NPs	4-mercaptobenzoic acid	-	Cu^{2+}	2.5×10^{-8}	UV-visible	[24]
Au NPs	Dithiocarbamate derivative of calixarene	14.0	Hg^{2+}	40 ppb	UV-visible	[25]
Au NPs	Mercaptopropionic acid and homocystine	4.0	Hg^{2+}	2 ppb	Cloud point extraction	[26]
Au NPs	Cyanuric acid	14.0	Hg^{2+}	-	UV-visible	[27]
Au NPs	Cysteamine	13-15	Hg^{2+} and melamine	30×10^{-9} and 80×10^{-9}	UV-visible	[28]
Au NPs	Thioctic acid	16.0	Hg^{2+}	10×10^{-9}	UV-visible	[29]
Au NPs	-	-	Cu^{2+}	250×10^{-9}	Click chemistry	[30]
Au NPs	Dopamine dithiocarbamate	5.0	Cu^{2+}	14.9×10^{-6}	UV-visible	[31]
Ag NPs	Cysteine	-	Cu^{2+} and Hg^{2+}	10×10^{-12} 1×10^{-12}	Surface enhanced Raman Scattering	[33]
Au NPs	Pyridines	3.0	Cu^{2+} and Ag^{+}	-	UV-visible	[34]
Ag NPs	Homocysteine	4-30	Cu^{2+} and Lidocaine hydrochloride	3.2×10^{-9} and 4.6×10^{-9}	Plasmon resonance scattering	[35]
Ag NCs	-	2.0	Hg^{2+} and Cu^{2+}	10×10^{-9}	Fluorescence	[36]
Au NPs	Protein	42	Hg^{2+} Pb^{2+} Cu^{2+}	200×10^{-9}	UV-visible	[38]
Au NPs	*L*-tyrosine	36 ± 2	Hg^{2+} Pb^{2+} Mn^{2+}	53×10^{-9} 16×10^{-9} -	UV-visible	[39]
Ag NPs	*L*-tyrosine	32 ± 2	Hg^{2+} Pb^{2+} Mn^{2+}	16×10^{-9} - 16×10^{-9}	UV-visible	[39]

Au NCs	Riboflavin	-	Cu^{2+}	0.9×10^{-6}	Fluorescence	[50]
Ag NPs	Starch	6.0	Cu^{2+}	0.5×10^{-6}	UV-visible	[51]
Au NPs	MA-DTC-Au NPs	20	Cu^{2+} Hg^{2+}	41×10^{-9} 45×10^{-9}	UV-visible	Present study

Table 2. MA-DTC-Au NPs as colorimetric probe for detection of Cu^{2+} and Hg^{2+} in water samples (drinking, tap, canal and river water).

Sample	Cu^{2+}				Hg^{2+}			
	Added (μM)	Found (μM)	Recovery (%) (*n*=3)	RSD (%) (*n*=3)	Added (μM)	Found (μM)	Recovery (%) (*n*=3)	RSD (%) (*n*=3)
Drinking	0.5	0.49	98.64	1.69	0.5	0.49	98.35	1.22
	5	4.96	99.21	1.24	5	4.95	99.10	1.75
	50	49.70	99.40	1.55	50	49.84	99.69	1.21
Tap	0.5	0.48	97.67	1.73	0.5	0.49	98.80	1.46
	5	4.91	98.22	1.52	5	4.92	98.56	1.92
	50	49.40	98.81	1.23	50	49.23	98.47	1.95
Canal	0.5	0.48	96.78	2.48	0.5	0.48	97.36	2.10
	5	4.88	97.70	2.70	5	4.82	96.43	2.61
	50	49.44	97.72	1.12	50	48.62	97.24	1.04
River	0.5	0.48	97.61	1.82	0.5	0.49	99.79	1.82
	5	4.89	97.97	2.02	5	4.92	98.53	2.52
	50	49.23	98.47	1.01	50	49.09	98.19	2.72

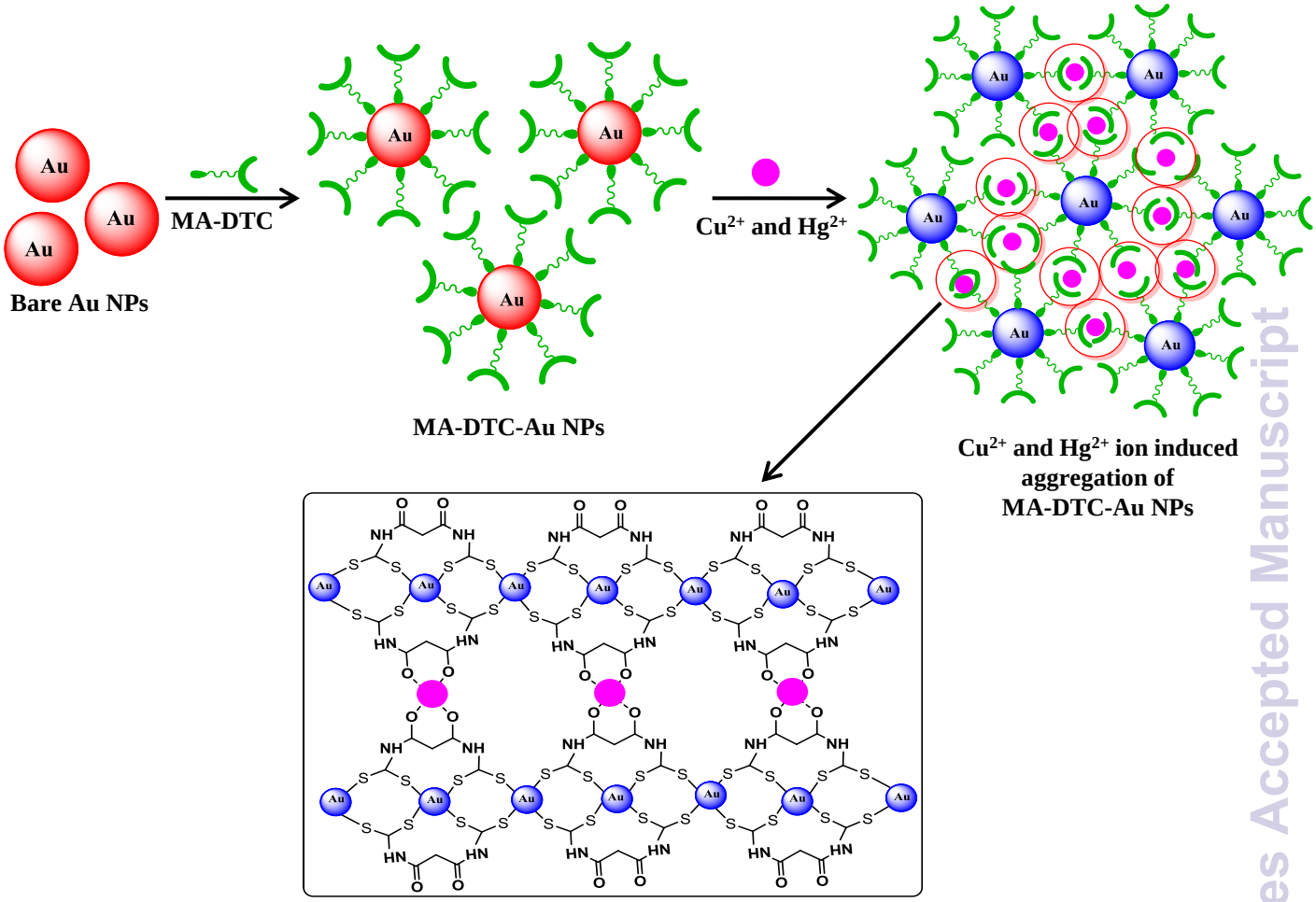

Scheme 1

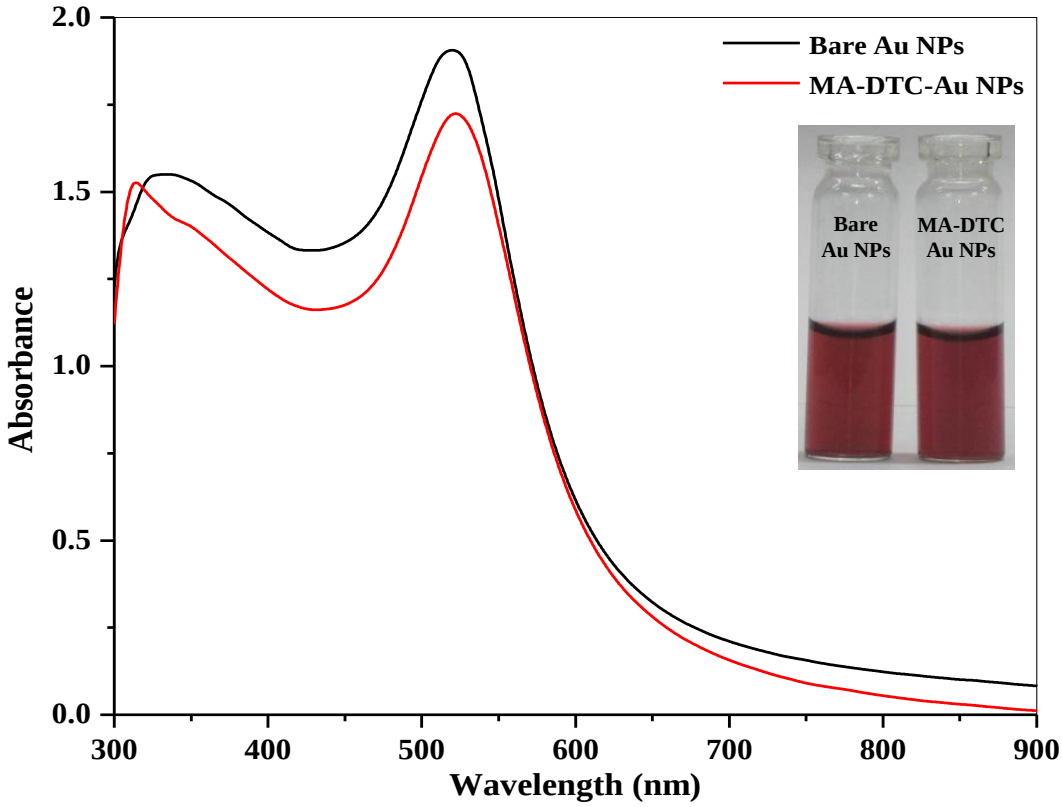

Figure 1

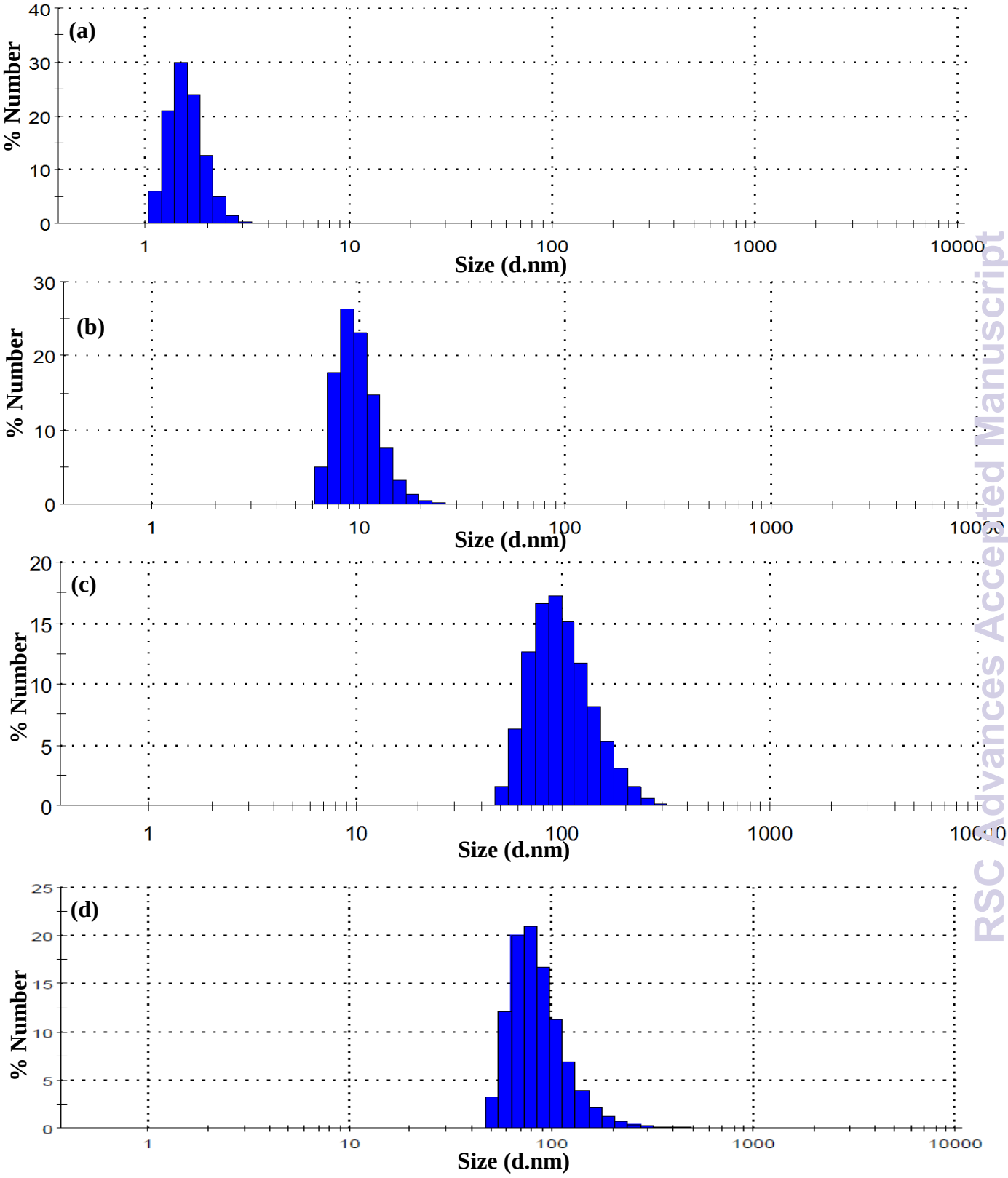

Figure 2

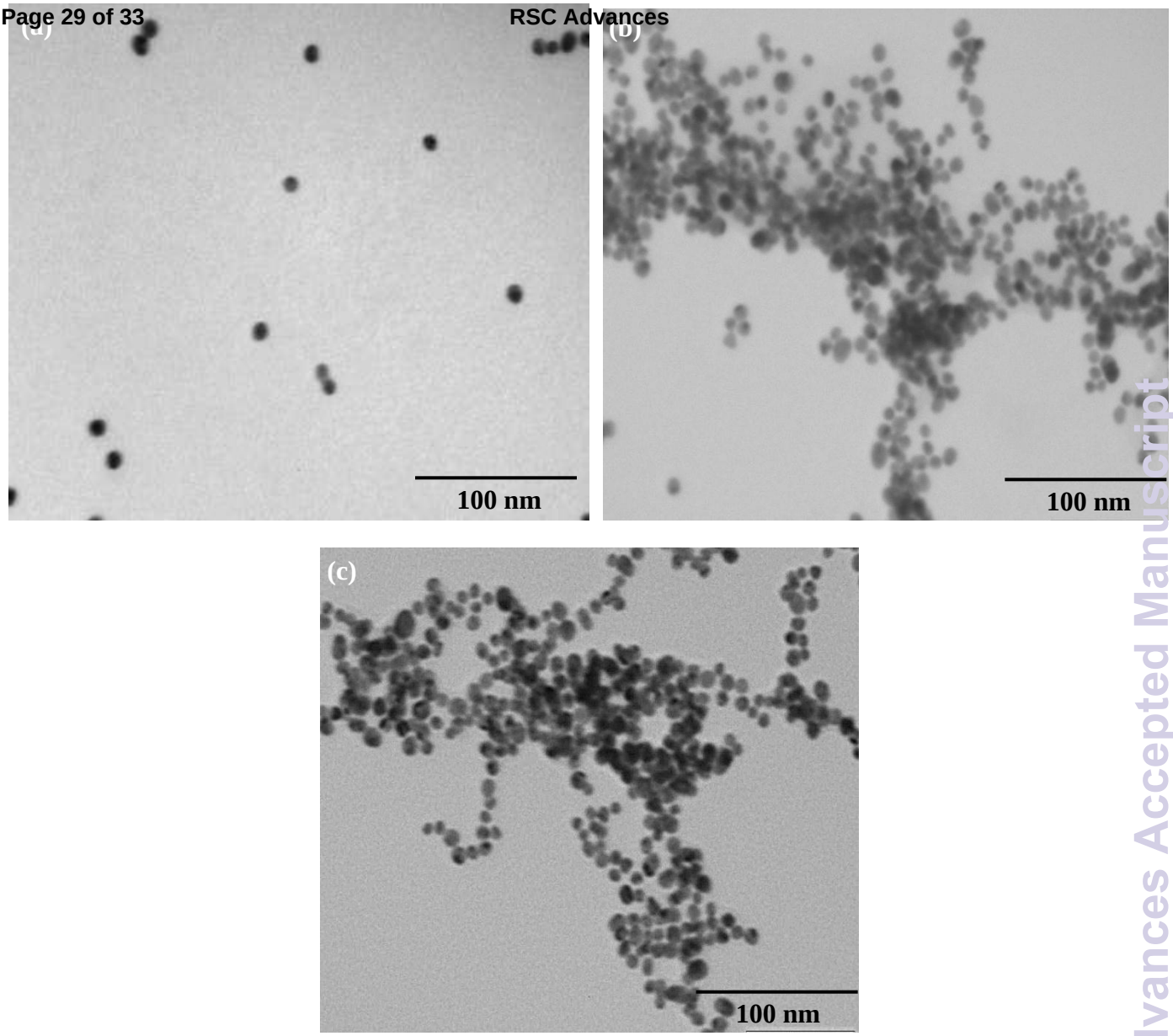

Figure 3

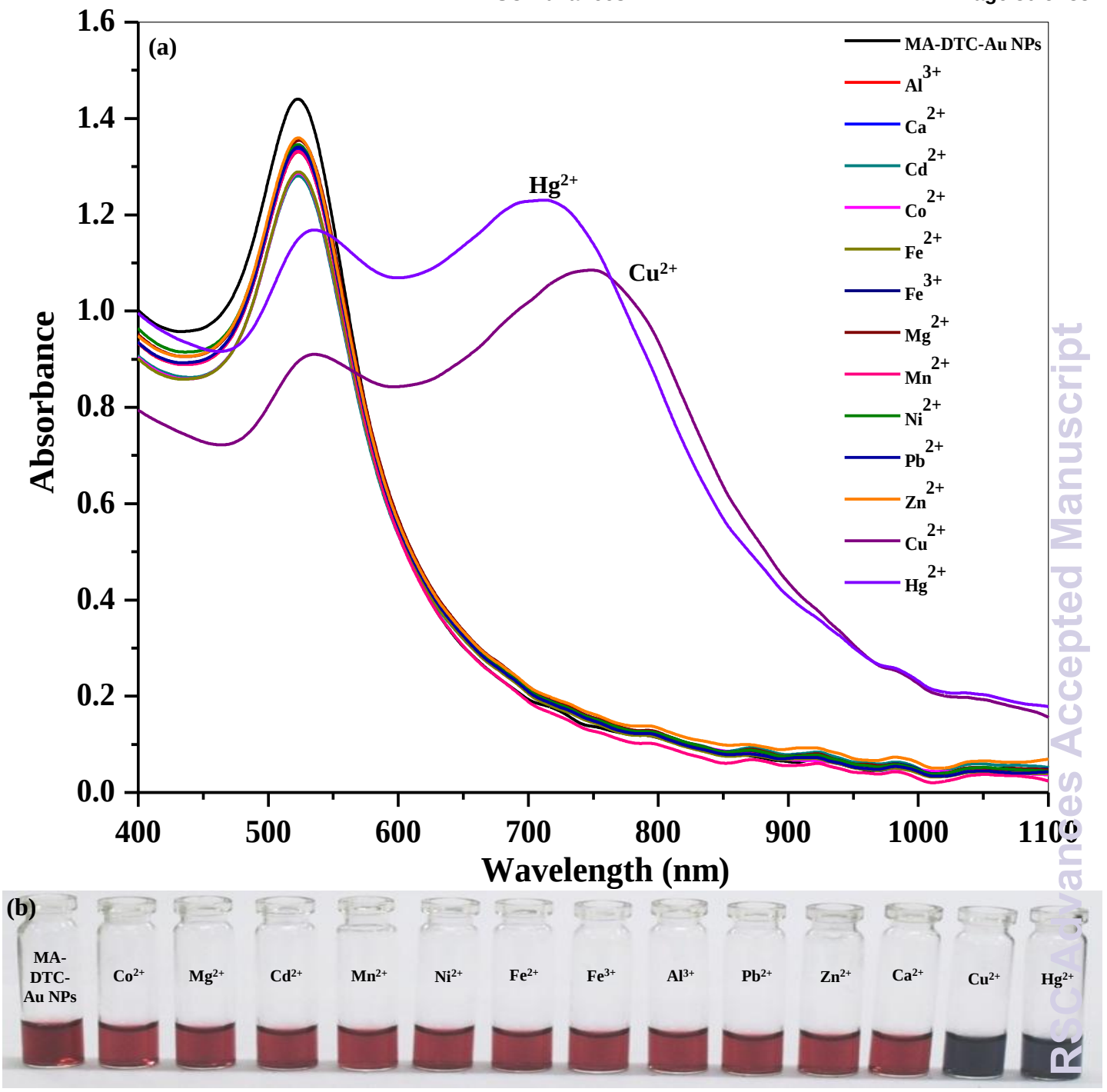

Figure 4

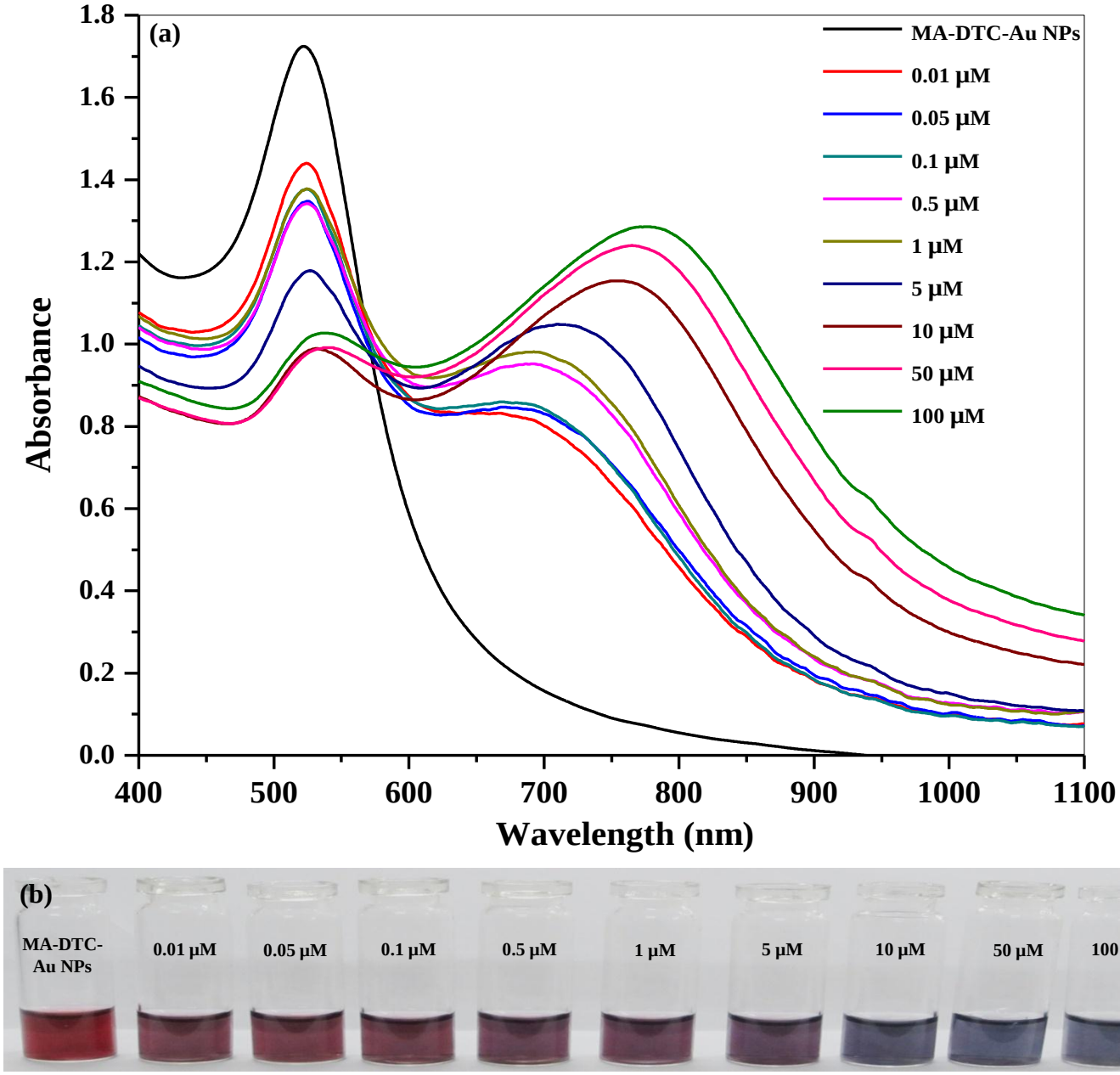

Figure 5

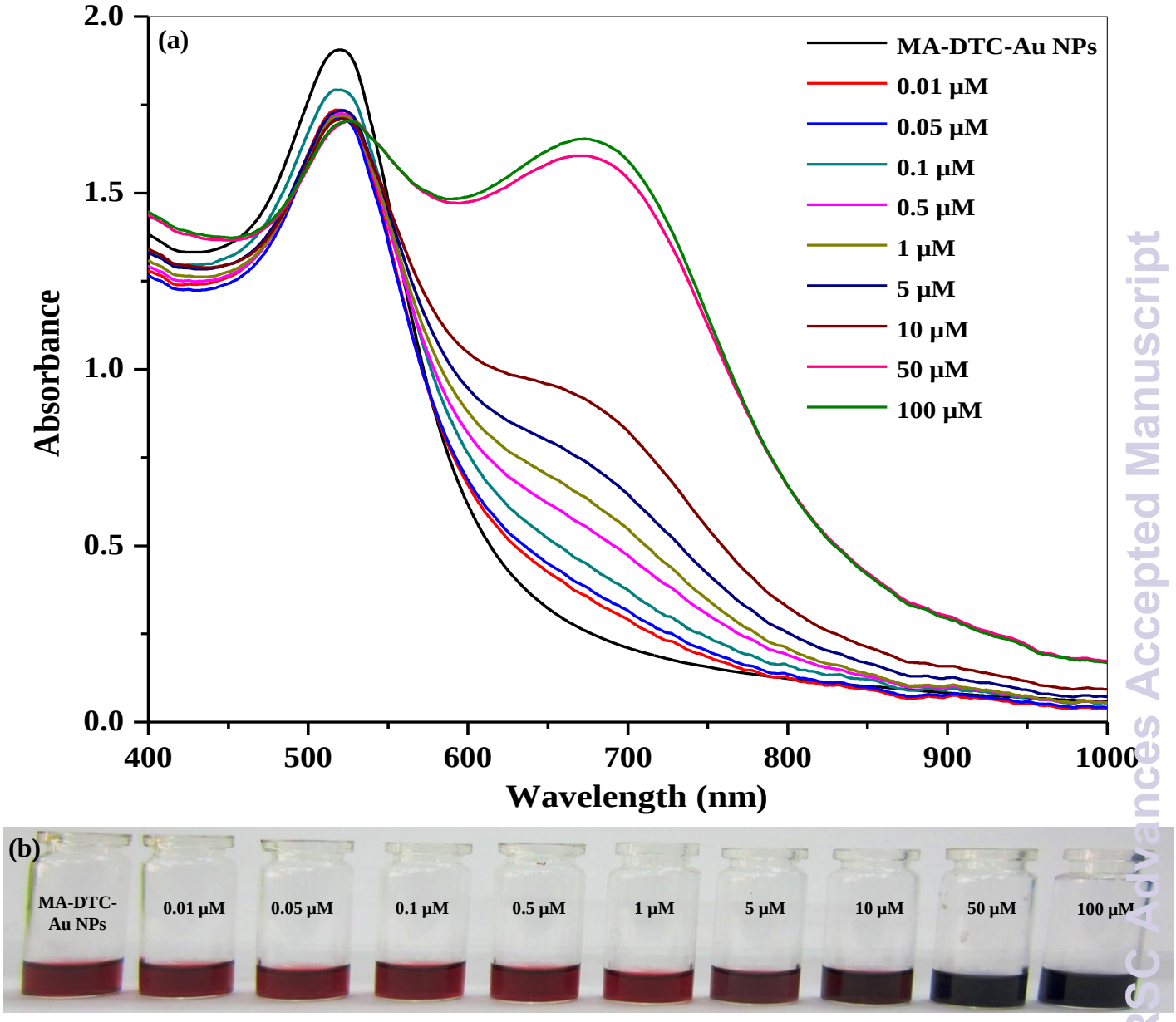

Figure 6

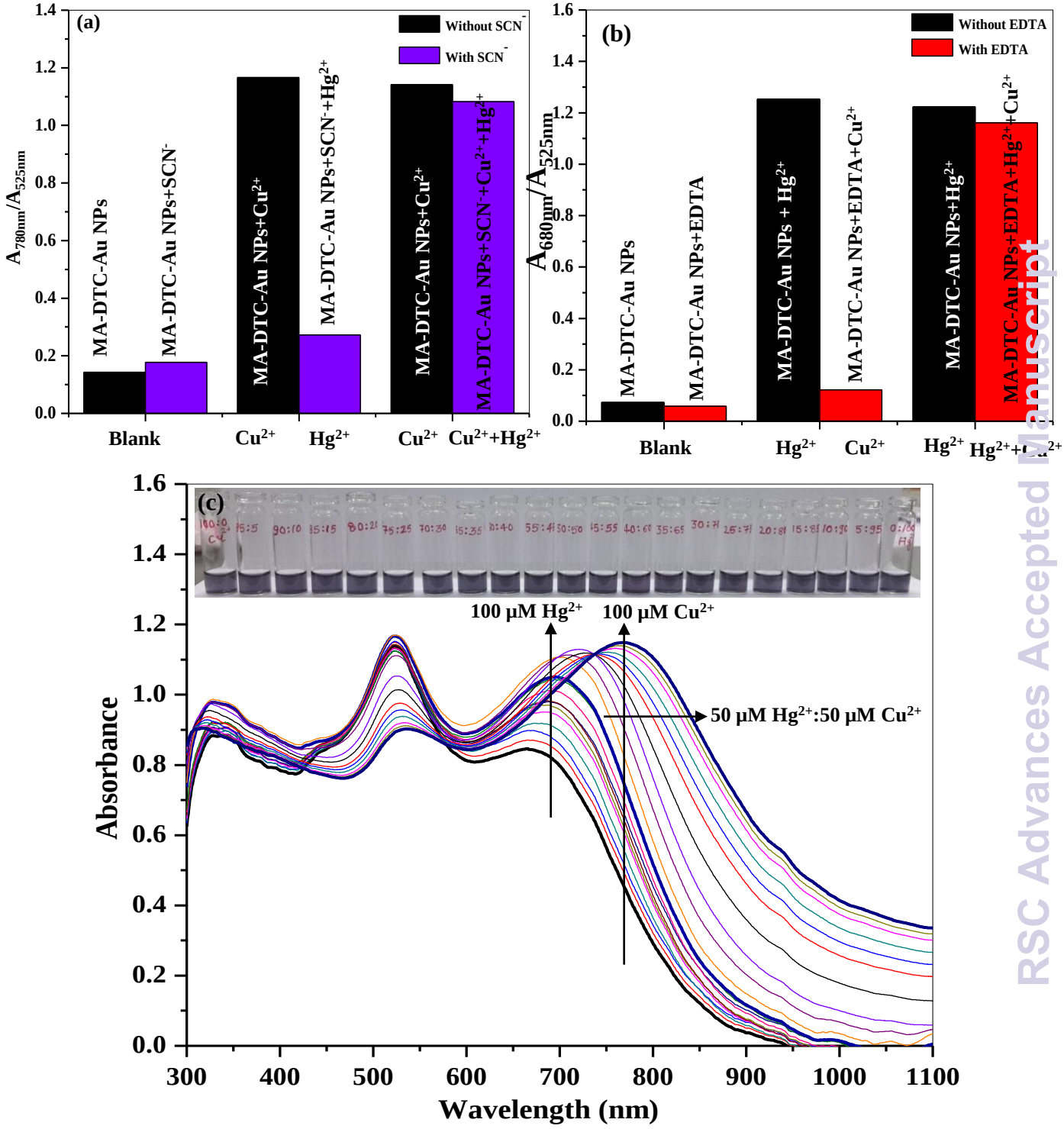

Figure 7.